

The effects of electronic structure and charged state on thermodynamic properties: An *ab initio* molecular dynamics investigations on neutral and charged clusters of Na₃₉, Na₄₀, and Na₄₁

Seyed Mohammad Ghazi,^{a)} Mal-Soon Lee, and D. G. Kanhere
*Department of Physics and Center for Modeling and Simulation, University of Pune,
 Ganeshkhind, Pune 411 007, India*

(Received 7 December 2007; accepted 8 January 2008; published online 12 March 2008)

In this paper we explore the effects of the electronic structure, the charge state, and the nature of energy distribution of isomers on the thermodynamic properties of sodium clusters. The focus of the work is to isolate the effects of these ingredients on thermodynamic behavior by choosing specific clusters. Toward this end we investigate Na₃₉⁻, Na₄₀, and Na₄₁⁺, which are the electronic closed shell systems which differ in number of atoms and charge state. We also examine Na₃₉, Na₃₉⁺, Na₄₀⁺, and Na₄₁ clusters having different charges of these clusters. Our density functional molecular dynamics simulations show that all electronic shell-closing clusters have similar melting temperature of ≈310 K. Remarkably, it is observed that an addition of even one electron to Na₃₉ increases the melting temperature by about 40 K and makes the specific heat curve sharper. All the cationic clusters show broadened specific heat curves. © 2008 American Institute of Physics.
 [DOI: 10.1063/1.2839278]

I. INTRODUCTION

The phase transformation in atomic clusters is a subject of considerable interest. During the last decade or so a number of issues pertaining to the melting phenomenon have been brought out by detailed experiments^{1,2} on free sodium clusters and a number of simulations using classical interatomic potentials^{3–8} as well as first principles molecular dynamics.^{9–20} Recent experiments on clusters of gallium and aluminum also show striking size sensitive behavior.^{21,22} Interpretation and understanding of the experimental observations such as size sensitive nature of the shapes of specific heat curves, irregular behavior of melting temperatures involves a delicate interplay of electronic structure, geometry, and influence of isomers. Further, even though all the experiments are carried out on charged clusters, a majority of theoretical simulations have been done on neutral clusters. Much less work dealing with the effect of charge on the thermodynamic properties has been reported.^{11,13}

In the present work we elucidate the effect of charge on the thermal properties of small sodium clusters. There is another interest concerning the effect of electronic structure and the ground-state geometry on thermodynamics of the cluster. It must be recognized that, in general, the electronic structure influences the nature of the ground state which in turn dictates the energy distribution of isomers. Thus it is not easy to isolate these effects. Therefore we have chosen to work on clusters of sodium around Na₄₀. These include Na₃₉⁻, Na₄₀, and Na₄₁⁺ to bring out the effect of electronic shell closing. In addition to these clusters, we also studied Na₃₉, Na₃₉⁺, Na₄₀⁺, and Na₄₁ to investigate the influence of the

charge state. The choice of these clusters also allows us to investigate the change in the geometry and its influence on the thermodynamics due to the additional one or two atoms, i.e., Na₃₉ to Na₄₁. We probe the thermodynamic properties with well established molecular dynamics methods and hope to bring out the effects of the electronic structure, charged state, isomers, and the ground-state geometry separately. In our previous works on sodium clusters we have examined the systematics of thermal properties from Na₈ to Na₅₈. We have been able to establish in these simple jelliumlike clusters a relationship between the nature of the ground-state geometry and the shape of the heat capacity. In almost all of these clusters it was not easy to discern the influence of electronic structure and the ground-state geometry separately except in the case of Na₅₅ and Na₅₈ (see also Ref. 11). Our results revealed that when a cluster has ordered structure as its ground-state geometry, it shows a sharp melting transition which is also seen in Ga clusters,²³ and an electronically closed shell system has a high melting temperature.²⁰ The present work also brings out the importance of the energy distribution of isomers in analyzing the thermal data. In this connection we mention the work of Bixon and Jortner,²⁴ where a simple model has been presented and as we shall see our results are consistent with their work. Finally, we note an interesting recent work by Noya *et al.* dealing with relationship of geometric magic numbers with the melting behavior of large sodium clusters.²⁵

In the next section (Sec. II) we give the computational details. Section III presents equilibrium geometries and their shape systematics followed by Sec. IV presenting the finite temperature behavior of these clusters. We conclude our discussion in Sec. V.

^{a)}Also at Ministry of Science, Research and Technology, Tehran, Iran. Electronic mail: mohammad@physics.unipune.ernet.in.

II. COMPUTATIONAL DETAILS

We have carried out Born–Oppenheimer molecular dynamics simulations²⁶ using Vanderbilt’s ultrasoft pseudopotentials²⁷ within the local-density approximation,²⁸ as implemented in the VASP package.²⁹ In order to get an insight into the evolutionary pattern of the geometries, we have obtained equilibrium structures for Na_{39}^- , Na_{39}^+ , Na_{39} , Na_{40} , Na_{40}^+ , Na_{41} , and Na_{41}^+ clusters. Among the above clusters, Na_{40} , Na_{39}^- and Na_{41}^+ are closed shell systems having 40 valence electrons. In each of the cases we have obtained about 200 different isomers. The initial configurations for the optimization were obtained from different *ab initio* constant temperature runs at different temperatures, near and above the melting point of the clusters.

The thermodynamic data are obtained from the molecular dynamical trajectories at constant temperature using Noe–Hoover³⁰ thermostat. We have used at least 10–12 different temperatures for each the cluster in the range of $120 \leq T \leq 400$ K. For each temperature the trajectory data are collected for period of at least 240 ps. We have discarded at least first 30 ps for thermalization. The resulting ionic trajectory data have been used to obtain multiple histograms. We have also analyzed various thermodynamics indicators such as Lindemann criteria (δ_{rms}) and mean square displacements (MSDs).

The shape of the ground-state geometry plays a crucial role in understanding the thermodynamics properties of cluster. We have used a shape deformation parameter ε_{def} to analyze the shape of the ground-state geometry for all the clusters. The deformation parameter ε_{def} is defined as

$$\varepsilon_{\text{def}} = \frac{2Q_x}{Q_y + Q_z}, \quad (1)$$

where $Q_x \geq Q_y \geq Q_z$ are the eigenvalues, in descending order, of the quadrupole tensor

$$Q_{ij} = \sum_I R_{iI} R_{jI}. \quad (2)$$

Here i and j run from 1 to 3, I runs over the number of ions, and R_{iI} is the i th coordinate of ion I relative to the cluster center of mass. We note that ε_{def} will be unity for a spherical cluster ($Q_x = Q_y = Q_z$). The configuration is said to be prolate when $Q_x \gg Q_y \approx Q_z$ and oblate when $Q_x \approx Q_y \gg Q_z$. A general completely asymmetric distribution of atoms is characterized by $Q_x \neq Q_y \neq Q_z$.

To analyze the thermodynamic properties, we first calculate the ionic specific heat by using the multiple histogram (MH) technique.^{31–33} We extract the classical ionic density of states ($\Omega(E)$) of the system, or equivalently the classical ionic entropy, $S(E) = k_B \ln \Omega(E)$, following the MH technique. In the canonical ensemble, the specific heat is defined as usual by $C(T) = \partial U(T) / \partial T$, where $U(T) = \int E p(E, T) dE$ is the average total energy. The probability of observing an energy E at a temperature T is given by the Gibbs distribution $p(E, T) = \Omega(E) \exp(-E/k_B T) / Z(T)$, with $Z(T)$ the normalized canonical partition function. We normalize the calcu-

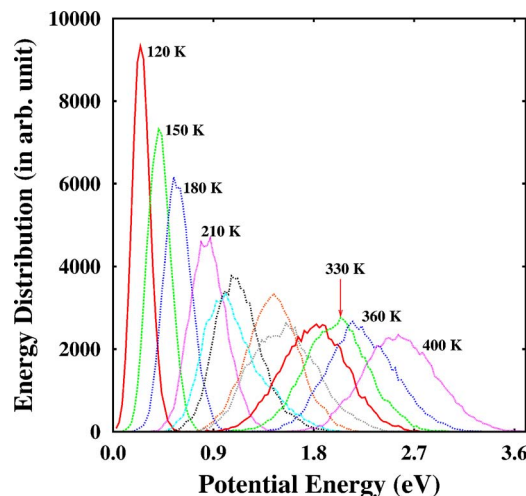


FIG. 1. (Color online) The distribution of the potential energy as a function of energy for Na_{39}^+ is shown.

lated canonical specific heat by the zero-temperature classical limit of the rotational plus vibrational specific heat, i.e., $C_0 = (3N - 6/2)k_B$.

A typical multiple histogram, i.e., the potential energy distribution spanned by the cluster at all the temperatures is shown in Fig. 1 for the case of Na_{39}^+ . The temperatures range from 120 to 400 K and have been chosen so as to have substantial overlap in the distributions. It may be noted from the figure that the normalized potential energy distribution for low temperatures is very sharp and narrow, indicating that the potential energy of the cluster changes very little. Indeed at low temperature the atoms exhibiting oscillatory motion around their equilibrium positions. At higher temperatures the bonds begin to break and the clusters span a much wider potential energy landscape, leading to a broad distribution. This rather broad potential energy distribution seen around 330 K and above as compared to the potential energy distribution for lower temperatures is suggestive of liquidlike nature of the cluster in this range of temperatures.

The Lindemann criteria δ_{rms} is defined as

$$\delta_{\text{rms}} = \frac{2}{N(N-1)} \sum_{i>j} \frac{(\langle r_{ij}^2 \rangle_t - \langle r_{ij} \rangle_t^2)^{1/2}}{\langle r_{ij} \rangle_t}, \quad (3)$$

where N is the number of atoms in the system, r_{ij} is the distance between atoms i and j , and $\langle \dots \rangle_t$ denotes a time average over the entire trajectory. It is convenient to define MSDs for individual atoms as

$$\langle \mathbf{r}_I^2(t) \rangle = \frac{1}{M} \sum_{m=1}^M [\mathbf{R}_I(t_{0m} + t) - \mathbf{R}_I(t_{0m})]^2, \quad (4)$$

where \mathbf{R}_I is the position of the I th atom and we average over M different time origins t_{0m} spanning over the entire trajectory. The interval between the consecutive t_{0m} for the average was taken to be about 1.5 ps. The MSDs of a cluster indicate the displacement of atoms in the cluster as a function of time.

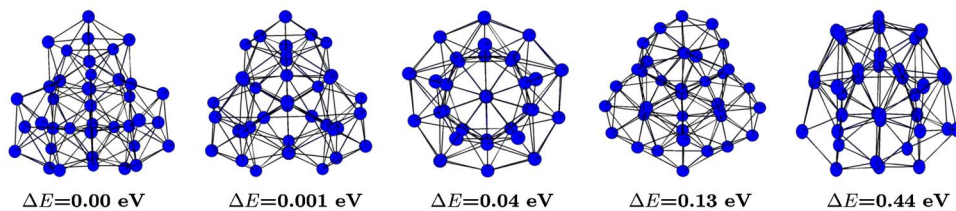
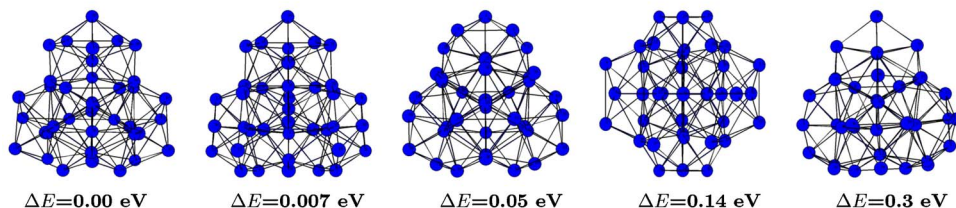
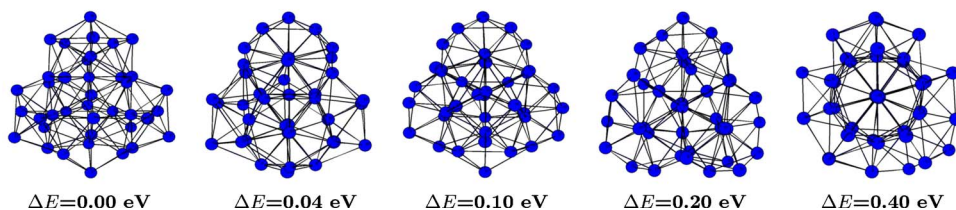
Na₃₉Na₃₉⁻Na₃₉⁺

FIG. 2. (Color online) The ground-state geometry and some of the representative isomers of clusters of Na₃₉⁻, Na₃₉, and Na₃₉⁺. ΔE represents the energy difference with respect to the ground state.

III. GEOMETRIES

The ground-state (GS) geometries and some representative isomers for all the clusters studied are shown in Figs. 2–4. In all the cases the isomer energies shown are relative to the energies of their ground states. The first isomer shown is found to be the closest in energy to the ground state. As can be seen in Fig. 2 the ground-state geometries of all 39 atom clusters consist of three nearly identical interpenetrating icosahedral units placed symmetrically. In fact, such icosahedral motifs dominate many isomers although some high-energy isomers show substantial distortion. The shape of Na₃₉⁻ is very similar to that of Na₃₉. Interestingly Na₃₉⁺ obtained by removing of one electron disturbs the structure showing a cap at the bottom (Fig. 2). It can be seen in Fig. 3 that the geometry of Na₄₀ is based on icosahedral structure

with missing 12 corner atoms and (111) facet as reported by Rytkönen *et al.*⁹ The additional atom added to Na₄₀, i.e., Na₄₁, is accommodated on the surface (and not as a cap) distorting the structure of Na₄₀ locally (Fig. 4). The examination of isomers reveals some interesting features. As we mentioned earlier a majority of the isomers of all the clusters show icosahedral motifs. The low-lying isomers of Na₃₉ have structure similar to the ground state of Na₄₀ and the structure of those for Na₄₀ and Na₄₁ clusters resembles the ground state of Na₃₉. It has been pointed out that the energy distribution of isomers has a significant role to play in a finite temperature properties.²⁴ We will examine and discussed the isomer energy distribution in conjunction with the thermodynamic properties.

In order to analyze the ground-state geometries in more

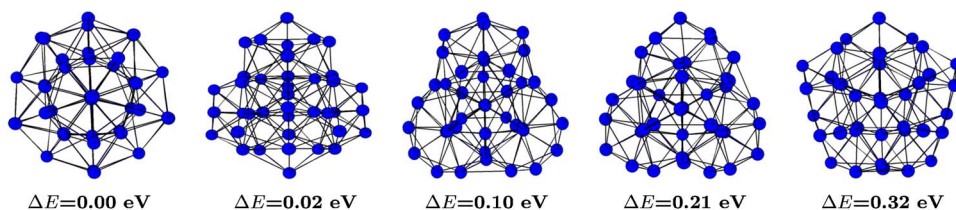
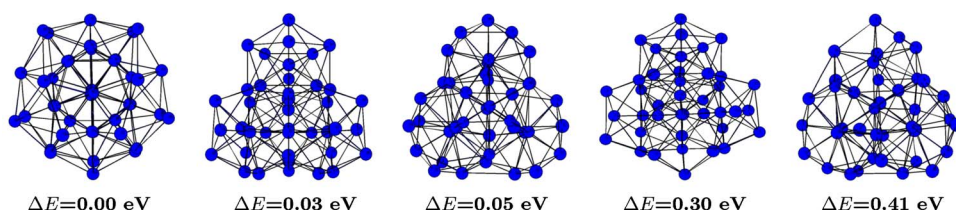
Na₄₀Na₄₀⁺

FIG. 3. (Color online) The ground-state geometry and some of the representative isomers of clusters of Na₄₀ and Na₄₀⁺. ΔE represents the energy difference with respect to the ground state.

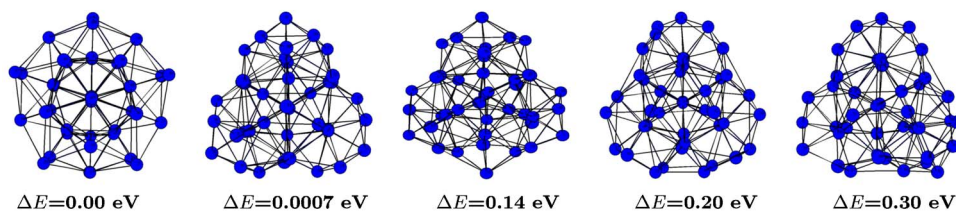
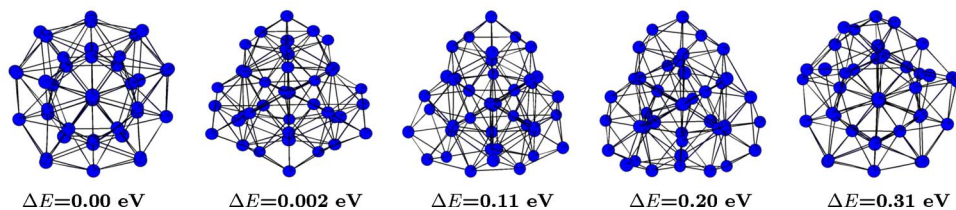
Na_{41}  Na_{41}^+ 

FIG. 4. (Color online) The ground-state geometry and some of the representative isomers of clusters of Na_{41} and Na_{41}^+ . ΔE represents the energy difference with respect to the ground state.

detail we present the shape deformation parameter ε_{def} , along with the three eigenvalues of quadrupole tensor [see Eqs. (1) and (2)], the distribution of the atoms from the center of mass and the distribution of the bond lengths for all the bonds in these clusters. We compare and contrast the differences in the nature of the ground state with the help of these parameters. Figure 5 shows the shape deformation parameter as a function of size for each of the cases. The maximum distortion from the spherical shape is observed in Na_{39}^+ having largest ε_{def} . While Na_{39}^- is the most symmetric cluster with the lowest value for ε_{def} (≈ 1). It can also be observed that the removal of one electron from all the neutral clusters has noticeable effect on their shapes. A closer examination of shapes shows that the ground states of all the clusters are slightly prolate.

The evolution of the partial formation of shell structure can be seen from Fig. 6 where we have shown the distances of all the atoms from the center of mass arranged in the increasing fashion. Among 39 atom clusters Na_{39}^- shows a clear shell-like arrangement displaying two main shells. Interestingly, Na_{39}^+ shows a nearly continuous distribution indicating that this cluster has no particular radial shell formation. The other clusters in the series fall in between these two extremes. It can be noticed that all cationic clusters become more disordered compared to their neutral clusters. This effect, namely, the ordering of atoms with the addition of two

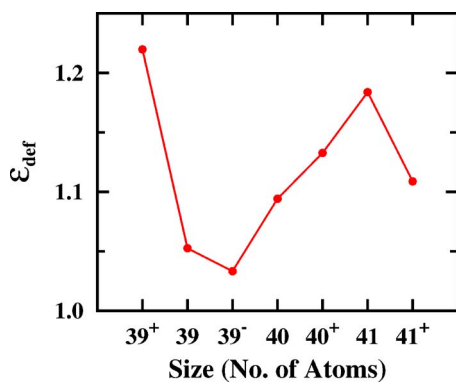


FIG. 5. (Color online) The shape deformation parameter for clusters as a function of size for the ground states.

electrons can also be seen by examining the distribution of the bondlength in these two clusters. In Fig. 7, we show the lowest hundred bond lengths where the x -axis enumerates the number of bond (in increasing order) and the y -axis gives the corresponding bondlength. The removal of charges from Na_{39} disturbs the steplike structure giving nearly continuous-bondlength distribution. Although the rearrangement of atoms is small, the effect is to bring in disorder in Na_{39}^+ .

Thus, our analysis of the GS geometries brings out two facts. First, charge state of the cluster influences the nature of the order in the GS (e.g., Na_{39}^+ to Na_{39}^-). Second, the cationic clusters have more disordered GS geometry compared to those of the neutral ones. It is interesting to note that electronic shell closing can be effected either by adding an atom or by adding an electron to Na_{39} . In the first case there is substantial change in the geometry while in the second case there is a subtle rearrangement of atoms. As we shall see both these closed shell systems will show very similar heat capacity curves. In addition to the structural properties, we also investigate the electronic structure of these clusters. To-

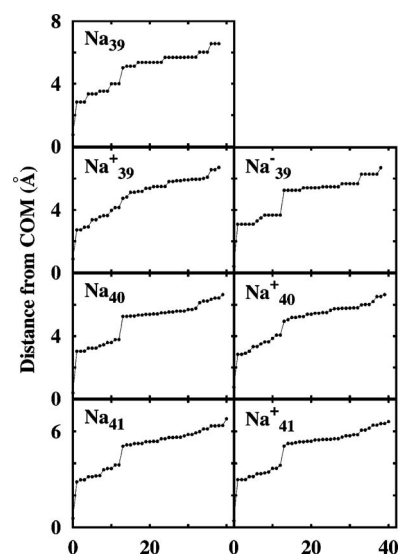


FIG. 6. The distance from the center of mass for each atom ordered in the increasing fashion for the ground states of studied clusters. The formation of shell is evident from the sharp steps.

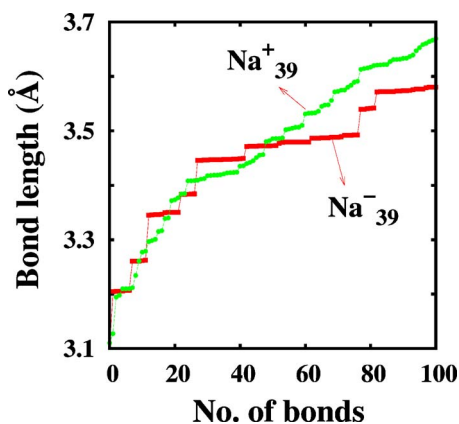


FIG. 7. (Color online) The distribution of bondlength in the increasing fashion for the first 100 numbers of bonds.

ward this end we show eigenvalue spectra in Fig. 8. It can be seen that the highest occupied molecular orbital (HOMO) and the lowest unoccupied molecular orbital (LUMO) vary substantially (of the order of ≈ 0.3 eV), the highest being for Na₃₉⁻. The effect of the change in the geometry is reflected in the nature of eigenvalue spectra shown in Fig. 8, although the main features of all the spectrum looks similar, confirming to the jellium pattern. The most symmetric cluster Na₃₉⁻ shows a relatively compact and nearly degenerate spectrum. More specifically “the bands” corresponding to *p, d, ...* label show strong bunching or near degeneracies. We anticipate a strong correlation between the nature of the ground state as revealed in these discussions and the specific heat to be presented and discussed in the next section.

IV. THERMODYNAMICS

The normalized heat capacity for all the clusters are shown in Fig. 9. The melting temperature is identified with the temperature at which peak occurs. A close examination of these curves brings out many interesting features. The melting temperature of Na₃₉⁻ is higher than that of Na₃₉ by

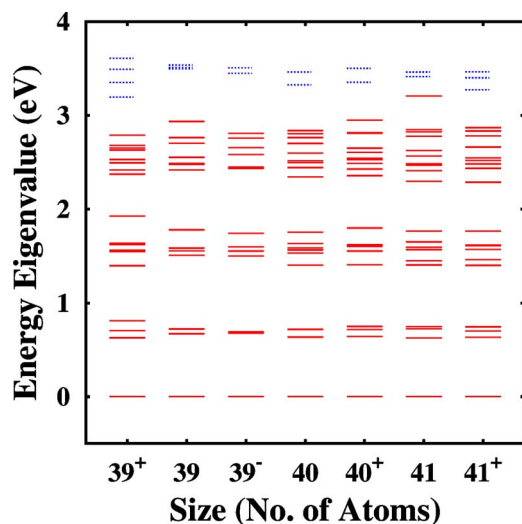


FIG. 8. (Color online) The eigenvalue spectra of the ground-state geometries as a function of cluster size, where solid lines show the occupied orbitals and dotted shorter lines show the unoccupied ones.

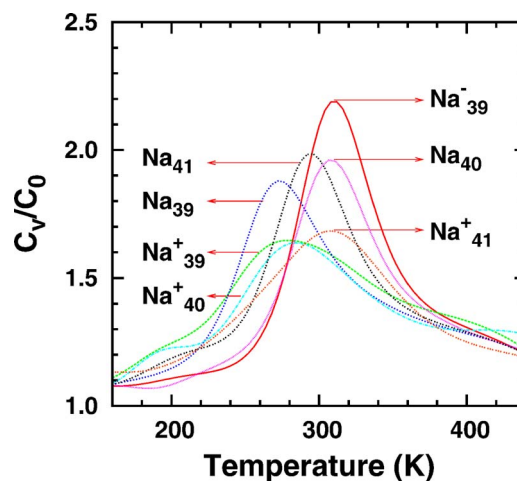


FIG. 9. (Color online) The normalized heat capacity curves for all the studied clusters.

40 K and the curve is noticeably sharper. Thus, an addition of even one electron changes the nature of the specific heat significantly. On the other hand, the removal of one electron from Na₃₉ makes the specific heat significantly broader without changing the melting temperature. Interestingly all the 40 electron systems, i.e., Na₄₀, Na₃₉⁻, and Na₄₁⁺, exhibit the same melting temperature of about 310 K.

It is remarkable that simple jelliumlike clusters which differ by 1 or 2 electrons or by 1 or 2 atoms show diverse nature in their thermal behavior. Most of the above observations can be understood on the basis of electronic structure, the charged state, energy spectrum of the isomers, and the nature of the ground-state geometries. We recall that there is hardly any difference in the ground-state geometries of Na₃₉ and Na₃₉⁻. However, an addition of one electron results in the completion of the electronic shell yielding the highest HOMO-LUMO gap. Therefore we attribute the increase in the melting temperature to the electronic structure, specially to the electronic shell-closing effect. This is also consistent with the fact that all closed shell clusters show the same melting temperature. This is a clear example of a change in the thermal behavior solely due to the change in the electronic structure. It may be noted that an addition of one atom to Na₃₉ changes both, the electronic structure and the geometry. Both these effects are manifested in the specific heat curve of Na₄₀. In other words, in Na₄₀ more ordered GS geometry results in the sharper peak and the electronic shell-closing affects its melting temperature to be higher.

Now we turn to the effect of the ordering of the GS geometry and charge sensitive features seen in the Fig. 9. It is most instructive to discuss these features by taking a specific example of the pair Na₃₉⁻ (sharply peaked specific heat) and Na₃₉⁺ (relatively broad specific heat) which shows the maximum contrast. There are two crucial properties, which influence the shapes, namely, the order or the extent of the order in the ground-state geometry and the energy distribution of isomers. Our earlier works on clusters of gallium²³ and sodium^{15,20,34} have clearly shown that a cluster having ordered geometry shows a sharp melting transition, while a cluster having a disordered geometry exhibits a broad tran-

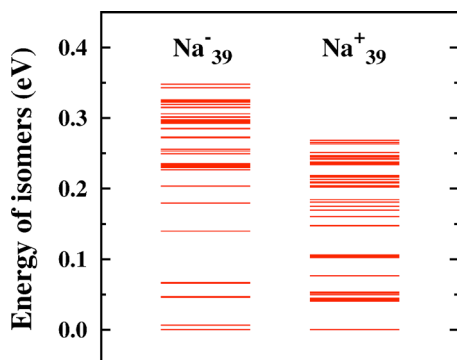


FIG. 10. (Color online) The isomer energy distribution relative to ground-state energy for the first 50 isomers in Na_{39}^- , and Na_{39}^+ .

sition. It may also be noted that the specific heat is directly influenced by the (ionic) energy spectrum. As pointed out by Bixon and Jortner²⁴ such a spectrum is characterized by the distribution of energies of the local minima of the ionic potential energy hypersurface. There are two inherent energy scales: Δ being the gap between the local minima and W being the energy spread of the excited-state structures around the local minima. Bixon and Jortner have presented a simple but transparent model correlating the nature of isomer spectrum and the shapes of the specific heat curves. They have shown that the width of the transition in the caloric curve (and further specific heat curve) is broadened with the increase of W/Δ . It is instructive to examine the isomer distribution of Na_{39}^- and Na_{39}^+ in the light of their work. In Fig. 10 we show the energy distributions for the first 50 low-energy isomers. It can be seen that the spectrum of Na_{39}^- is significantly more gaped with small energy spread. This is the case where $\Delta \gg W$. The spectrum for Na_{39}^+ shows less gaps with bigger spread leading to an increase of W/Δ . Thus, the sharper peaked nature of the heat capacity curve in Na_{39}^- is consistent with the analysis of Bixon and Jortner. The broad nature of the curve for Na_{39}^+ is due to hierarchical isomerization.²⁴

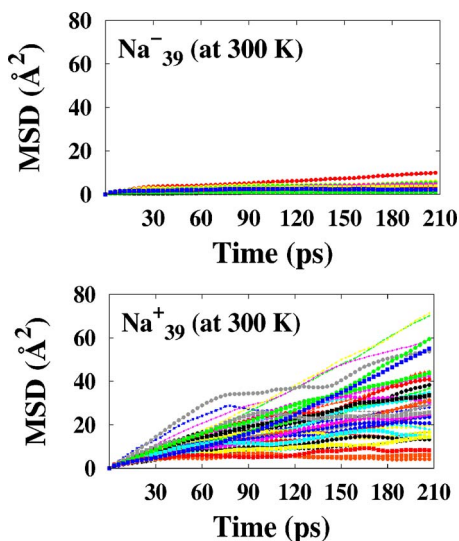


FIG. 11. (Color online) The comparison of the mean-square displacements (MSDs) of individual atoms at 300 K for Na_{39}^- and Na_{39}^+ computed over 210 ps.

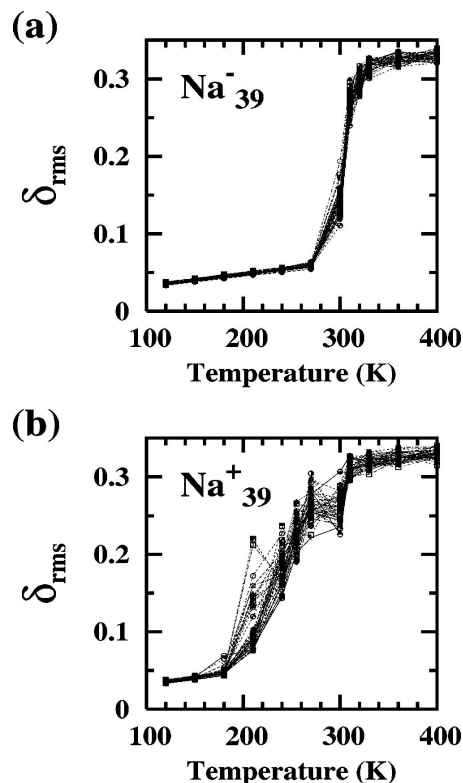


FIG. 12. The δ_{rms} of individual atoms for (a) Na_{39}^- and (b) Na_{39}^+ .

The broadness of specific heat curve can be also examined by calculating the mean square displacements (MSDs) and Lindemann criteria, i.e., root-mean-square bond length fluctuations (δ_{rms}) for these two representative clusters. Our discussion so far brings out the fact that the atoms in Na_{39}^+ are bounded to rest of the cluster with different strengths and therefore they will respond differently (with different amplitudes). The behavior of mean square displacement is shown in Fig. 11. The contrast in the response of atoms in these two clusters to temperature is evident. At 300 K almost all the atoms in Na_{39}^- are exhibiting small oscillations giving rise to very small mean square displacements. The MSD values for Na_{39}^+ show a wide range from 5 to 60 \AA^2 , indicating widely different response of individual atoms. This behavior is typical of clusters showing broad specific heat curve. This is also reflected in the Lindemann criteria (δ_{rms}) calculated for each atom (Fig. 12). It can be seen that in Na_{39}^- all the atoms “melt” together while in the case of Na_{39}^+ a clear spread is seen.

There is another interesting observation seen in Fig. 9. All the cationic clusters studied, i.e., Na_{39}^+ , Na_{40}^+ , and Na_{41}^+ , show significantly broader specific heat curves as compared to the rest. The melting temperatures of the cationic clusters are also different from their neutral ones. Since all the experiments are performed on charged clusters, it is prudent to be cautious while comparing the results of simulations with the experiments.

V. SUMMARY AND CONCLUSION

The *ab initio* molecular dynamical simulations have been employed to probe the finite temperature properties of

sodium clusters having number of atoms equal to 39, 40, and 41. The heat capacities of anionic, neutral, and cationic clusters have been calculated and discussed in order to bring out the effect of geometry, electronic structure, charge state, and the isomer energy distribution. In general, it is not easy to discern the influence of electronic structure and geometry on the thermal properties separately. In the present case we have been able to isolate these effects by careful choice of the clusters chosen around Na₄₀. Our results show that the nature of the heat capacities, i.e., the shape and melting temperature, can change significantly if the cluster changes from anionic to cationic. We show that the increase in the melting temperature due to addition of extra electrons in Na₃₉ is purely an electronic structure effect. In addition our results bring out the effect of energy distribution of isomers on the shapes of heat capacity curves. We believe that by and large such an energy distribution is influenced by the nature of the ground-state geometries. For example, the cluster having highly symmetric, well ordered ground state will show spectrum with a large gap in a low energy region leading to a sharp peak. In contrast to this the isomer states of a cluster having disordered ground state may even be gapless.³⁴

ACKNOWLEDGMENTS

We acknowledge partial assistance from the Indo-French center for Promotion of Advance Research (India)/Center Franco-Indian pour la promotion de la Recherche Avancée (France) (IFC-PAR, Project No. 3104-2). One of the authors (S.M.G.) acknowledges financial support from the Indian Council for Cultural Relations (ICCR). It is a pleasure to thank Shahab Zorriasatein and Kavita Joshi for a number of useful discussions.

¹M. Schmidt, R. Kusche, B. von Issendorff, and H. Haberland, *Nature (London)* **393**, 238 (1998); R. Kusche, Th. Hippler, M. Schmidt, B. V. Issendorff, and H. Haberland, *Eur. Phys. J. D* **9**, 1 (1999); M. Schmidt, R. Kusche, Th. Hippler, J. Donges, W. Kronmüller, B. V. Issendorff, and H. Haberland, *Phys. Rev. Lett.* **86**, 1191 (2001); M. Schmidt and H. Haberland, *C. R. Phys.* **3**, 327 (2002).

²M. Schmidt, J. Donges, Th. Hippler, and H. Haberland, *Phys. Rev. Lett.* **90**, 103401 (2003); H. Haberland, Th. Hippler, J. Donges, O. Kostko, M. Schmidt, and B. von Issendorff, *ibid.* **94**, 035701 (2005).

³Y. Li, E. Blaisten-Barojas, and D. A. Papaconstantopoulos, *Phys. Rev. B* **57**, 15519 (1998).

⁴F. Calvo and F. Spiegelmann, *Phys. Rev. Lett.* **82**, 2270 (1999).

⁵F. Calvo and F. Spiegelmann, *J. Chem. Phys.* **112**, 2888 (2000).

⁶F. Calvo and F. Spiegelmann, *J. Chem. Phys.* **120**, 9684 (2004).

⁷J. A. Reyes-Neva, I. L. Garzon, M. R. Beltran, and K. Michaelian, *Rev. Mex. Fis.* **48**, 450 (2002); J. A. Reyes-Neva, I. L. Garzon, and K. Michaelian, *Phys. Rev. B* **67**, 165401 (2003).

⁸K. Manninen, A. Rytönen, and M. Manninen, *Eur. Phys. J. D* **29**, 39 (2004).

⁹A. Rytönen, H. Häkkinen, and M. Manninen, *Phys. Rev. Lett.* **80**, 3940 (1998).

¹⁰A. Rytönen, H. Häkkinen, and M. Manninen, *Eur. Phys. J. D* **9**, 451 (1999).

¹¹K. Manninen, H. Häkkinen, and M. Manninen, *Phys. Rev. A* **70**, 023203 (2004).

¹²K. Manninen, T. Santa-Nokki, H. Häkkinen, and M. Manninen, *Eur. Phys. J. D* **34**, 43 (2005).

¹³K. Manninen, H. Häkkinen, and M. Manninen, *Comput. Mater. Sci.* **35**, 158 (2006).

¹⁴S. Chacko, D. G. Kanhere, and S. A. Blundell, *Phys. Rev. B* **71**, 155407 (2005).

¹⁵M.-S. Lee, S. Chacko, and D. G. Kanhere, *J. Chem. Phys.* **123**, 164310 (2005).

¹⁶A. Aguado and J. M. López, *Phys. Rev. Lett.* **94**, 233401 (2005).

¹⁷A. Aguado and J. M. López, *Phys. Rev. B* **74**, 115403 (2006).

¹⁸M. Itoh, V. Kumar, and Y. Kawazoe, *Phys. Rev. B* **73**, 035425 (2006).

¹⁹O. Kostko, B. Huber, M. Moseler, and B. von Issendorff, *Phys. Rev. Lett.* **98**, 043401 (2007).

²⁰M.-S. Lee and D. G. Kanhere, *Phys. Rev. B* **75**, 125427 (2007).

²¹A. A. Shvartsburg and M. F. Jarrold, *Phys. Rev. Lett.* **85**, 2530 (2000); G. A. Breaux, R. C. Benirschke, T. Sugai, B. S. Kinnear, and M. F. Jarrold, *ibid.* **91**, 215508 (2003).

²²G. A. Breaux, D. A. Hillman, C. M. Neal, R. C. Benirschke, and M. F. Jarrold, *J. Am. Chem. Soc.* **126**, 8628 (2004); G. A. Breaux, C. M. Neal, B. Cao, and M. F. Jarrold, *Phys. Rev. Lett.* **94**, 173401 (2005).

²³K. Joshi, S. Krishnamurty, and D. G. Kanhere, *Phys. Rev. Lett.* **96**, 135703 (2006).

²⁴M. Bixon and J. Jortner, *J. Chem. Phys.* **91**, 1631 (1989).

²⁵E. G. Noya, J. P. K. Doye, and D. J. Wales, and A. Aguado, *Eur. Phys. J. D* **43**, 57 (2007).

²⁶M. C. Payne, M. P. Teter, D. C. Allan, T. A. Arias, and J. D. Joannopoulos, *Rev. Mod. Phys.* **64**, 1045 (1992).

²⁷D. Vanderbilt, *Phys. Rev. B* **41**, 7892 (1990).

²⁸P. Hohenberg and W. Kohn, *Phys. Rev.* **136**, B864 (1964); W. Kohn and L. J. Sham, *Phys. Rev.* **140**, A1133 (1965).

²⁹Vienna *ab initio* simulation package, Technische Universität Wien (1999); G. Kresse and J. Furthmüller, *Phys. Rev. B* **54**, 11169 (1996).

³⁰S. Nošé, *Prog. Theor. Phys. Suppl.* **103**, 1 (1991).

³¹A. M. Ferrenberg and R. H. Swendsen, *Phys. Rev. Lett.* **61**, 2635 (1988).

³²P. Labastie and R. L. Whetten, *Phys. Rev. Lett.* **65**, 1567 (1990).

³³P. Chandrachud, K. Joshi, and D. G. Kanhere, *Phys. Rev. B* **76**, 235423 (2007).

³⁴S. Zorriasatein, M.-S. Lee, and D. G. Kanhere, *Phys. Rev. B* **76**, 165414 (2007).